

Leptogenesis assisted by scalar decays

Jun-Yu Tong, Zhao-Huan Yu,^{*} and Hong-Hao Zhang[†]

School of Physics, Sun Yat-Sen University, Guangzhou 510275, China

We present a pragmatic approach to lower down the mass scale of right-handed neutrinos in leptogenesis by introducing a scalar decaying to right-handed neutrinos. The key point of our proposal is that the out-of-equilibrium decays of the scalar provide an additional source for right-handed neutrinos and hence the lepton asymmetry. This mechanism works well at low temperatures when the washout of the generated lepton asymmetry is suppressed. Thus, the lepton asymmetry can be effectively produced despite the washout effect is strong or not. Through a comprehensive analysis, we demonstrate that such a scalar-assisted leptogenesis can typically decrease the viable right-handed neutrino mass scale by one to three orders of magnitude.

CONTENTS

I. Introduction	2
II. Model	3
III. Boltzmann equations	7
IV. Parameter scans	15
V. Summary	16
Acknowledgments	18
References	18

^{*} Corresponding author. yuzhaoh5@mail.sysu.edu.cn

[†] Corresponding author. zh98@mail.sysu.edu.cn

I. INTRODUCTION

Although matter and antimatter are treated symmetrically in particle physics and quantum field theory, stars and galaxies in the celestial neighborhood are constituted exclusively by baryonic matter. Actually, a matter-antimatter symmetric observable universe is excluded by the observation of the cosmic diffuse γ -ray background [1]. The baryon asymmetry of the universe is conventionally quantified by the net baryon-to-photon number density $\eta_B = (n_B - n_{\bar{B}})/n_\gamma$. Combining the observations of the cosmic microwave background by the Planck collaboration [2] and the primordial abundances of light elements related to big bang nucleosynthesis, η_B is determined to be [3]

$$\eta_B = (6.13 \pm 0.04) \times 10^{-10}. \quad (1)$$

In order to generate such a baryon asymmetry, the related physical processes must satisfy three Sakharov conditions [4], i.e., the violation of the baryon number B , the C and CP violations, and the departure from thermal equilibrium. The standard model (SM) by itself could fulfill all the three conditions. The B violation occurs through a nonperturbative effect in electroweak interactions known as the sphaleron processes [5, 6], and the interactions out of thermal equilibrium may happen in a strong first-order electroweak phase transition. This makes electroweak baryogenesis [7] a promising mechanism to generate the baryon asymmetry. However, subsequent researches reveal that the electroweak phase transition in the SM is just a smooth crossover because the Higgs boson mass is too large [8–10]. Thus, a successful baryogenesis can only take place in new physics beyond the SM. Some comprehensive reviews can be found in Refs. [11–13].

Among new physics theories trying to explain the origin of the baryon asymmetry, leptogenesis [14, 15] is a well-motivated mechanism related to the tiny masses of active neutrinos. It typically introduces three generations of heavy right-handed neutrinos (RHNs), allowing active neutrinos to acquire Majorana masses through the type-I seesaw mechanism [16–18]. The decays of RHNs give rise to the lepton asymmetry, which is subsequently converted into the baryon asymmetry via the sphaleron processes. Such a leptogenesis mechanism can be realized in various models (see Refs. [19–35] for an incomplete list of recent works).

Nevertheless, the standard thermal leptogenesis typically requires a high mass scale of the RHNs. For achieving an adequate CP violation in RHN decays, the lightest RHN mass should be larger than 10^9 GeV [36]. Moreover, the generated lepton asymmetry would be strongly washed out if the RHN Yukawa couplings are too large [37–39]. Taking into account the washout effect and the neutrino oscillation data, it demands the lightest RHN mass to be at least $\sim 10^{10}$ GeV for obtaining the correct baryon-to-photon ratio [37]. Such a high mass scale is challenging to be further tested by experiments.

In order to circumvent a strong washout effect and/or lower down the RHN mass scale, several solutions were proposed. One solution is to assume leptogenesis originating from the reheating process after inflation [40–42]. Another approach is to reprocess CP -violating interactions at

high scales into the $B - L$ asymmetry by RHN interactions at lower scales, known as wash-in leptogenesis [43, 44]. Additional avenues include considering nonthermal particle production from the evaporation of primordial black holes [45–49], imposing restrictions on the related couplings [50, 51], embedding leptogenesis within a first-order phase transition [52], and assuming nonstandard cosmology [53, 54]. Besides, a lower RHN mass scale can also be achieved by resonant leptogenesis [55–60], flavored leptogenesis [61–63], and extra CP -violation by an additional scalar [64].

Motivated by these efforts, we propose another approach to decrease the RHN mass scale by introducing a scalar boson ϕ that decays into RHNs when the ϕ particles are out of thermal equilibrium¹. We assume a slow decay rate of ϕ to ensure the continuous production of RHNs, even when the washout processes are suppressed at low temperatures. Thus, it provides an additional nonthermal source for the lepton asymmetry. By tracking the particle number density evolution in this scenario, we will explore the suitable parameter regions that can effectively lower down the lightest RHN mass.

The paper is structured as follows. In Section II, we introduce our model, which extends the SM by incorporating a scalar field and three RHNs, and outline the calculations of the CP asymmetry and the requisite decay widths and scattering cross sections. Section III is dedicated to analyzing the Boltzmann equations and number densities to assess the efficacy of the model. In Section IV, we explore the viable parameter regions by performing parameter scans. Finally, we conclude this work in Section V.

II. MODEL

We extend the SM with three generations of RHNs N_{iR} ($i = 1, 2, 3$) and a real scalar ϕ , which is an SM gauge singlet. The CP -violating decays of the RHNs are expected to give rise to an asymmetry in the lepton number L . The related Lagrangian is

$$\begin{aligned}
 -\mathcal{L} \supset & \left(h_{\nu,ij} \overline{L_{iL}} \tilde{H} N_{jR} + \frac{1}{2} M_{N_i} \overline{N_{iR}^c} N_{iR} + \frac{1}{2} y_i \overline{N_{iR}^c} N_{iR} \phi + \text{H.c.} \right) \\
 & + m_\phi^2 \phi^2 + \kappa H^\dagger H \phi + \lambda_{\phi H} H^\dagger H \phi^2.
 \end{aligned} \tag{2}$$

Here L_{iL} represent the $SU(2)_L$ doublets of the left-handed leptons, and $\tilde{H} = i\sigma_2 H^*$ is the iso-doublet of the SM Higgs field

$$H = \begin{pmatrix} H^+ \\ H^0 \end{pmatrix}, \tag{3}$$

which develops a vacuum expectation value $v = 174$ GeV, leading to the spontaneous breaking of the electroweak gauge symmetry. N_{iR} carry no $U(1)_Y$ charges and weakly couple to the real scalar ϕ via the Yukawa couplings y_i . N_{iR}^c are the charge conjugates of N_{iR} . The Yukawa couplings $h_{\nu,ij}$ give Dirac mass terms for the neutrinos after electroweak symmetry breaking,

¹ The impact of a scalar coupling to RHNs has also been studied in Refs. [65, 66] for other motivations.

while M_{N_i} provide Majorana mass terms. Among the couplings between ϕ and the SM Higgs doublet H , κ is a dimension-1 coupling constant, while $\lambda_{\phi H}$ is dimensionless. We assume that ϕ does not develop a nonzero vacuum expectation value and its mass is just given by m_ϕ .

After the electroweak symmetry breaking, the mass terms for the neutrinos become

$$-\mathcal{L}_{\text{mass}} = \frac{1}{2} \begin{pmatrix} \overline{\nu_L} & \overline{N_R^c} \end{pmatrix} \begin{pmatrix} 0 & v h_\nu \\ v h_\nu^T & M \end{pmatrix} \begin{pmatrix} \nu_L^c \\ N_R \end{pmatrix}, \quad (4)$$

where $M = \text{diag}(M_{N_1}, M_{N_2}, M_{N_3})$ is the diagonal mass matrix for RHNs. Through a block-diagonalization of the 6×6 mass matrix in $\mathcal{L}_{\text{mass}}$, the 3×3 mass matrix for the active neutrinos is given by

$$M_\nu \simeq -v^2 h_\nu M^{-1} h_\nu^T \quad (5)$$

for $M \gg v h_\nu$. Thus, the large RHN masses give an origin to the tiny masses of the active neutrinos via the type-I seesaw mechanism. On the other hand, the flavor eigenstates of the RHNs basically coincide with their mass eigenstates, and three Majorana spinor fields can be constructed by $N_i = N_{iR}^c + N_{iR}$. The masses of the corresponding heavy Majorana neutrinos N_i are approximately given by M_{N_i} .

A specific form of the Yukawa coupling matrix h_ν can be derived by the Casas-Ibarra parametrization [67]. The active neutrino mass matrix M_ν , which is complex and symmetric, can be diagonalized by the unitary Pontecorvo–Maki–Nakagawa–Sakata (PMNS) matrix U [68, 69]:

$$U^T M_\nu U = M_\nu^d, \quad (6)$$

where $M_\nu^d = \text{diag}(m_1, m_2, m_3)$. Blending Eqs. (5) and (6), we have

$$-v^2 U^T h_\nu M^{-1} h_\nu^T U = M_\nu^d, \quad (7)$$

and it is not difficult to obtain

$$-v^2 \left[\left(\sqrt{M_\nu^d} \right)^{-1} U^T h_\nu \left(\sqrt{M} \right)^{-1} \right] \left[\left(\sqrt{M} \right)^{-1} h_\nu^T U \left(\sqrt{M_\nu^d} \right)^{-1} \right] = I_{3 \times 3}, \quad (8)$$

where the square root of a diagonal matrix means the square roots of its diagonal elements. Thus,

$$R^T \equiv -i v \left(\sqrt{M_\nu^d} \right)^{-1} U^T h_\nu \left(\sqrt{M} \right)^{-1} \quad (9)$$

must be a 3×3 complex orthogonal matrix satisfying $R^T R = I_{3 \times 3}$. Therefore, the Yukawa coupling matrix can be expressed as

$$h_\nu = \frac{i}{v} U^* \sqrt{M_\nu^d} R^T \sqrt{M}, \quad (10)$$

TABLE I. Three-flavor global fit results of neutrino oscillation parameters in 1σ range.

θ_{12} ($^\circ$)	θ_{23} ($^\circ$)	θ_{13} ($^\circ$)	δ_{CP} ($^\circ$)	Δm_{21}^2 (10^{-5} eV 2)	Δm_{31}^2 (10^{-3} eV 2)
$33.44^{+0.77}_{-0.74}$	$49.2^{+1.0}_{-1.3}$	$8.57^{+0.13}_{-0.12}$	194^{+52}_{-25}	$7.42^{+0.21}_{-0.20}$	$2.515^{+0.028}_{-0.028}$

which implies that larger values in the RHN mass matrix M leads to larger Yukawa couplings h_ν if the other parameters are fixed.

Following Particle Data Group's convention [70] for the parametrization of the PMNS matrix, we have

$$U = \begin{pmatrix} c_{12}c_{13} & s_{12}c_{13} & s_{13}e^{-i\delta_{CP}} \\ -s_{12}c_{23} - c_{12}s_{13}s_{23}e^{i\delta_{CP}} & c_{12}c_{23} - s_{12}s_{13}s_{23}e^{i\delta_{CP}} & c_{13}s_{23} \\ s_{12}s_{23} - c_{12}s_{13}c_{23}e^{i\delta_{CP}} & -c_{12}s_{23} - s_{12}s_{13}c_{23}e^{i\delta_{CP}} & c_{13}c_{23} \end{pmatrix} \begin{pmatrix} e^{i\eta_1} & 0 & 0 \\ 0 & e^{i\eta_2} & 0 \\ 0 & 0 & 1 \end{pmatrix}, \quad (11)$$

where $c_{ij} \equiv \cos \theta_{ij}$, $s_{ij} \equiv \sin \theta_{ij}$. δ_{CP} is the Dirac CP phase and $\eta_{1,2}$ are the Majorana CP phases. In the following calculation, we assume a normal hierarchy for the active neutrino masses, and set the Majorana phases to be zero and the neutrino oscillation parameters to be the best fit values from the global analysis given by the NuFIT collaboration [71], which are listed in Table I.

Moreover, we assume the lightest neutrino mass m_1 to be zero, leading to $m_2 = \sqrt{\Delta m_{21}^2}$ and $m_3 = \sqrt{\Delta m_{31}^2}$. In this case, the complex orthogonal matrix R can be described by a single complex parameter $z = z_r + iz_i$ [72] with a form of

$$R = \begin{pmatrix} 0 & \cos z & \sin z \\ 0 & -\sin z & \cos z \\ 1 & 0 & 0 \end{pmatrix}. \quad (12)$$

for the normal hierarchy. Thus, given the values of m_{N_1} , m_{N_2} , m_{N_3} , z_r , and z_i , the Yukawa coupling matrix h_ν can be determined through Eq. (10).

The CP asymmetry in the decays of the heavy Majorana neutrino N_i to light leptons and Higgs bosons can be measured by

$$\varepsilon_i = \frac{\Gamma(N_i \rightarrow \ell H) - \Gamma(N_i \rightarrow \bar{\ell} \bar{H})}{\Gamma(N_i \rightarrow \ell H) + \Gamma(N_i \rightarrow \bar{\ell} \bar{H})}, \quad (13)$$

where $\ell = \ell_j^-, \nu_j$ ($j = 1, 2, 3$) and $H = H^+, H^0$, while $\bar{\ell}$ and \bar{H} represent their antiparticles. Considering the interference of one-loop diagrams with tree-level diagrams, it is given by [73]

$$\varepsilon_i = \frac{1}{8\pi} \sum_{j \neq i} \left[f\left(\frac{M_{N_j}^2}{M_{N_i}^2}\right) - \frac{M_{N_i} M_{N_j}}{M_{N_j}^2 - M_{N_i}^2} \right] \frac{\text{Im}\{[(h_\nu^\dagger h_\nu)_{ij}]^2\}}{(h_\nu^\dagger h_\nu)_{ii}}, \quad (14)$$

where $f(x) = \sqrt{x}\{1 - (1+x)\ln[(1+x)/x]\}$. Basically, ε_i are positively correlated to the Yukawa couplings $h_{\nu,ij}$, which are positively correlated to M_{N_i} as mentioned above. When the

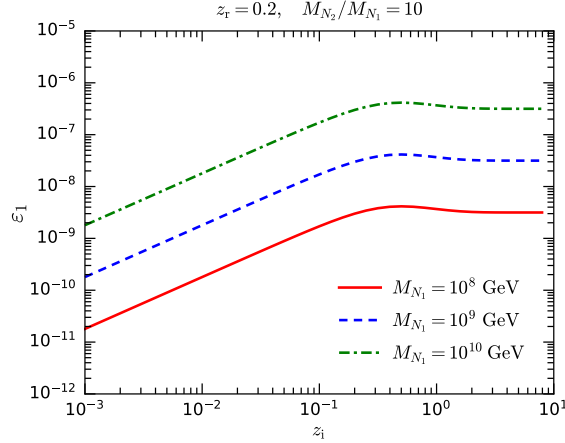


FIG. 1. The CP asymmetry ε_1 as functions of z_i for $M_{N_1} = 10^8, 10^9$, and 10^{10} GeV with $z_r = 0.2$, $M_{N_2} = 10M_{N_1}$, and $M_{N_3} \rightarrow \infty$.

CP -violating N_i decays are out of thermal equilibrium, a lepton number asymmetry would be generated.

In Fig. 1, we demonstrate the CP asymmetry in the N_1 decays as functions of z_i for $M_{N_1} = 10^8, 10^9$, and 10^{10} GeV. The other parameters are fixed as $z_r = 0.2$, $M_{N_2} = 10M_{N_1}$, and $M_{N_3} \rightarrow \infty$. It is evident that the CP asymmetry ε_1 is basically proportional to M_{N_1} . Moreover, ε_1 increases as z_i increases for $z_i \lesssim 0.4$, but it tends to be saturated for $z_i \gtrsim 0.4$.

For simplicity, we further assume a mass hierarchy of the heavy Majorana neutrinos as $M_{N_1} \ll M_{N_2}, M_{N_3}$. As a result, the lepton asymmetry generated by N_2 and N_3 will be washed out by the inverse decay processes $\ell H / \bar{\ell} \bar{H} \rightarrow N_1$. Therefore, only the $B-L$ numbers yielded from N_1 remain and are subsequently converted into the baryon asymmetry through the electroweak sphaleron processes [6]. This is the one-flavor approximation. After the electroweak crossover, the sphaleron processes freeze out, and the resulting baryon-to-photon ratio at recombination can be estimated as [12]

$$\eta_B = \frac{c_s}{f} \frac{n_{B-L}}{n_\gamma} \simeq 0.013 \frac{n_{B-L}}{n_\gamma}. \quad (15)$$

Here, n_{B-L} and n_γ represent the number densities of the $B-L$ charges and the photons, respectively. $c_s = 28/79$ is the conversion ratio of the $B-L$ asymmetry to the baryon asymmetry via the sphaleron processes for the inclusion of three RHNs [74]. $f = 2387/86$ is a dilution factor accounting for the increase in n_γ in a comoving volume from the epoch with $T \sim m_{N_1}$ to recombination.

The washout effect plays a crucial role in diminishing the final yield of n_{B-L} . The primary washout processes are the inverse decays $\ell H / \bar{\ell} \bar{H} \rightarrow N_1$. They are related to the decay width of N_1 , which is given by

$$\Gamma_{N_1} = \Gamma(N_1 \rightarrow \ell H) + \Gamma(N_1 \rightarrow \bar{\ell} \bar{H}) \simeq \frac{1}{8\pi} (h_\nu^\dagger h_\nu)_{11} M_{N_1}, \quad (16)$$

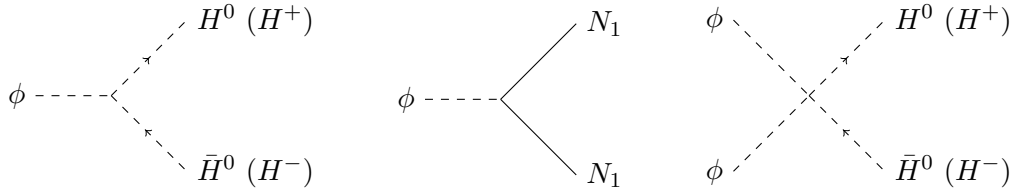


FIG. 2. Decay and scattering diagrams for the scalar ϕ .

where the masses of light leptons and Higgs bosons have been neglected.

In our scenario extending the standard leptogenesis, the additional real scalar ϕ could decay into RHNs. For simplicity, we assume a mass hierarchy of

$$2M_{N_1} < m_\phi < 2M_{N_2} \ll M_{N_3}, \quad (17)$$

which implies that ϕ can only decay into $N_1 N_1$ and $H \bar{H}$. The relevant decay and annihilation diagrams for ϕ are illustrated in Fig. 2. At tree level, the partial decay widths for $\phi \rightarrow N_1 N_1$ and $\phi \rightarrow H \bar{H}$ are

$$\Gamma(\phi \rightarrow N_1 N_1) = \frac{y_1^2 m_\phi}{16\pi} \left(1 - \frac{4M_{N_1}^2}{m_\phi^2}\right)^{3/2}, \quad (18)$$

$$\Gamma(\phi \rightarrow H \bar{H}) \simeq \frac{\kappa^2}{8\pi m_\phi}. \quad (19)$$

The annihilation cross sections for $\phi\phi \rightarrow H \bar{H}$ are given by

$$\sigma(\phi\phi \rightarrow H^0 \bar{H}^0) = \sigma(\phi\phi \rightarrow H^+ H^-) \simeq \frac{\lambda_{\phi H}^2}{4\pi s \sqrt{1 - 4m_\phi^2/s}}, \quad (20)$$

where s is a Mandelstam variable.

The ϕ decays into $N_1 N_1$ are followed by the subsequent N_1 decays, which give rise to the lepton asymmetry if the N_1 particles depart from thermal equilibrium. If the ϕ lifetime is sufficiently long, the production of N_1 particles persists even when the washout effect is suppressed at low temperatures. In the next section, we will provide a comprehensive analysis for the evolution of the lepton asymmetry.

III. BOLTZMANN EQUATIONS

In this section, we utilize a set of Boltzmann equations [12, 75, 76] to study the evolution of the number densities of the ϕ particles, the N_1 particles, and the $B - L$ charges, which are denoted by n_ϕ , n_{N_1} , and n_{B-L} , respectively. With the assumptions made in the previous section,

the Boltzmann equation for n_ϕ reads

$$\begin{aligned} \frac{dn_\phi}{dt} + 3Hn_\phi = & -\langle\Gamma_{\phi\rightarrow N_1 N_1}\rangle \left[n_\phi - \frac{n_\phi^{\text{eq}} n_{N_1}^2}{(n_{N_1}^{\text{eq}})^2} \right] - \langle\Gamma_{\phi\rightarrow H\bar{H}}\rangle (n_\phi - n_\phi^{\text{eq}}) \\ & - \langle\sigma_{\phi\phi\rightarrow H\bar{H}}v\rangle \left[n_\phi^2 - (n_\phi^{\text{eq}})^2 \right], \end{aligned} \quad (21)$$

where H is the Hubble expansion rate, and the collision terms are related to the $\phi \leftrightarrow N_1 N_1$, $\phi \leftrightarrow H\bar{H}$, and $\phi\phi \leftrightarrow H\bar{H}$ processes. n_i^{eq} indicate the number densities in thermal equilibrium, while $\langle\Gamma_i\rangle$ and $\langle\sigma_{\phi\phi\rightarrow H\bar{H}}v\rangle$ denote the thermal averages of the decay width Γ_i and the $\phi\phi \rightarrow H\bar{H}$ scattering cross section $\sigma_{\phi\phi\rightarrow H\bar{H}}$ multiplied by the Møller velocity, respectively.

Taking into account the $N_1 \leftrightarrow \ell H / \bar{\ell} \bar{H}$ and $\phi \leftrightarrow N_1 N_1$ processes, the Boltzmann equation for n_{N_1} is

$$\frac{dn_{N_1}}{dt} + 3Hn_{N_1} = -\langle\Gamma_{N_1}\rangle (n_{N_1} - n_{N_1}^{\text{eq}}) + \langle\Gamma_{\phi\rightarrow N_1 N_1}\rangle \left[n_\phi - \frac{n_\phi^{\text{eq}} n_{N_1}^2}{(n_{N_1}^{\text{eq}})^2} \right]. \quad (22)$$

Moreover, the evolution of n_{B-L} is governed by

$$\frac{dn_{B-L}}{dt} + 3Hn_{B-L} = -\varepsilon_1 \langle\Gamma_{N_1}\rangle (n_{N_1} - n_{N_1}^{\text{eq}}) - \frac{1}{2} \langle\Gamma_{N_1}\rangle \frac{n_{N_1}^{\text{eq}} n_{B-L}}{n_\ell^{\text{eq}}}, \quad (23)$$

where the first term in the right-hand side corresponds to the generation of the lepton asymmetry by the CP asymmetry ε_1 and the departure of the N_1 particles from thermal equilibrium, and the second term, which is proportional to n_{B-L} , indicates the washout of the generated lepton asymmetry caused by the inverse decays.

Note that the integrated Boltzmann equations (21)–(23) are derived from the full Boltzmann equations that govern the evolution of momentum distributions of particles [77–79], assuming that the ϕ and N_1 particles are in kinetic equilibrium with the SM plasma at the same temperature. This assumption ensures that the decay width or cross section of a process, along with the corresponding equilibrium number densities, can be used to describe the contribution of the inverse process. For instance, the contributions of $N_1 N_1 \rightarrow \phi$ and $H\bar{H} \rightarrow \phi\phi$ in Eq. (21) are given by $\langle\Gamma_{\phi\rightarrow N_1 N_1}\rangle n_\phi^{\text{eq}} n_{N_1}^2 / (n_{N_1}^{\text{eq}})^2$ and $\langle\sigma_{\phi\phi\rightarrow H\bar{H}}v\rangle (n_\phi^{\text{eq}})^2$, respectively. If the kinetic equilibrium is not maintained, the integrated Boltzmann equations cannot be expressed in such closed forms, and the full Boltzmann equations are more appropriate for obtaining precise results.

Once the ϕ particles are produced via the $H\bar{H} \rightarrow \phi\phi$ process at high temperatures $T \gg m_\phi$, they rapidly archive kinetic equilibrium through the scattering processes $\phi H \rightarrow \phi H$ and $\phi\bar{H} \rightarrow \phi\bar{H}$, primarily mediated by the quartic coupling $\lambda_{\phi H}$. Nonetheless, for low temperatures $T \lesssim m_\phi$, the kinetic equilibrium may no longer be maintained, and its condition must be carefully examined. The scattering cross section for $\phi H \rightarrow \phi H$ with nonrelativistic ϕ particles is given by

$$\langle\sigma_{\text{scat}}v\rangle \simeq \frac{\lambda_{\phi H}^2}{16\pi m_\phi^2}, \quad (24)$$

which leads to a scattering rate of $\Gamma_{\text{scat}} = 4n_H \langle \sigma_{\text{scat}} v \rangle$, accounting for the four degrees of freedom of the Higgs bosons. Based on analyses in Refs. [80–82], the condition for kinetic equilibrium can be approximated as

$$\frac{T}{m_\phi} \frac{\Gamma_{\text{scat}}}{H} \gtrsim 1, \quad (25)$$

where the suppression factor T/m_ϕ reflects the requirement of a sufficient number of scatterings to establish kinetic equilibrium.

For our scenario to be viable, the quartic coupling $\lambda_{\phi H}$ cannot be too large; otherwise, the annihilation process $\phi\phi \rightarrow H\bar{H}$ would excessively deplete the ϕ particles, rendering the nonthermal production of N_1 particles via ϕ decays inefficient. For the values of $\lambda_{\phi H}$ used in the following analysis, the condition (25) can hardly be satisfied for $T \lesssim m_\phi$. Consequently, at such low temperatures, the kinetic equilibrium of ϕ particles with the SM plasma breaks down. This implies that the contributions of the inverse processes $N_1 N_1 \rightarrow \phi$, $H\bar{H} \rightarrow \phi$, and $H\bar{H} \rightarrow \phi\phi$ no longer retain the closed forms presented in Eqs. (21) and (22). Nevertheless, these contributions are greatly suppressed for $T \ll m_\phi$, as the N_1 particles and Higgs bosons lack sufficient energy to produce ϕ particles. As a result, the integrated Boltzmann equations (21) and (22) still serve as credible approximations for $T \lesssim m_\phi$.

The kinetic equilibrium of N_1 particles is primarily maintained by the $1 \leftrightarrow 2$ processes $N_1 \leftrightarrow \ell H / \bar{\ell} \bar{H}$ and $\phi \leftrightarrow N_1 N_1$. In contrast to $2 \leftrightarrow 2$ processes, $1 \leftrightarrow 2$ processes are generally inefficient for achieving thermalization, rendering the assumption of kinetic equilibrium largely invalid [77–79]. Nevertheless, solutions to the full Boltzmann equations indicate that the resulting lepton asymmetry does not differ significantly from that obtained by solving the integrated Boltzmann equations. If one defines $K \equiv \Gamma_{N_1}/H(M_{N_1})$, where $H(M_{N_1})$ is the Hubble rate at $T = M_{N_1}$, the difference of the lepton asymmetry for $K > 5$ is less than 15% [77]. For the parameter points used in the subsequent analysis, the condition $K > 5$ is always satisfied. Therefore, the results and conclusions derived from solving the integrated Boltzmann equations (21)–(23) are expected to be reliable.

In order to separate the dynamical evolution from the cosmological expansion effect, it is more convenient to use the ratios of these number density to the photon number density, $Y_i = n_i/n_\gamma$. A dimensionless parameter $x = M_{N_1}/T$ is further introduced to replace the temperature T . Thus, the set of Boltzmann equations (21)–(23) can be transformed into a simplified form,

$$\begin{aligned} \frac{dY_\phi}{dx} = & -\frac{\langle \Gamma_{\phi \rightarrow N_1 N_1} \rangle}{Hx} \left[Y_\phi - \frac{Y_\phi^{\text{eq}} Y_{N_1}^2}{(Y_{N_1}^{\text{eq}})^2} \right] - \frac{\langle \Gamma_{\phi \rightarrow H\bar{H}} \rangle}{Hx} (Y_\phi - Y_\phi^{\text{eq}}) \\ & - \frac{n_\gamma \langle \sigma_{\phi\phi \rightarrow H\bar{H}} v \rangle}{Hx} [Y_\phi^2 - (Y_\phi^{\text{eq}})^2], \end{aligned} \quad (26)$$

$$\frac{dY_{N_1}}{dx} = -\frac{\langle \Gamma_{N_1} \rangle}{Hx} (Y_{N_1} - Y_{N_1}^{\text{eq}}) + \frac{\langle \Gamma_{\phi \rightarrow N_1 N_1} \rangle}{Hx} \left[Y_\phi - \frac{Y_\phi^{\text{eq}} Y_{N_1}^2}{(Y_{N_1}^{\text{eq}})^2} \right], \quad (27)$$

$$\frac{dY_{B-L}}{dx} = -\frac{\varepsilon_1 \langle \Gamma_{N_1} \rangle}{Hx} (Y_{N_1} - Y_{N_1}^{\text{eq}}) - \frac{\langle \Gamma_{N_1} \rangle Y_{N_1}^{\text{eq}}}{2Hx Y_\ell^{\text{eq}}} Y_{B-L}, \quad (28)$$

where $Y_i^{\text{eq}} \equiv n_i^{\text{eq}}/n_\gamma$. Based on the Friedmann equation, the Hubble rate H is determined by the energy densities of SM radiation, ϕ , and N_1 :

$$H^2 = \frac{8\pi}{3M_{\text{Pl}}^2}(\rho_{\text{R}} + \rho_\phi + \rho_{N_1}). \quad (29)$$

The SM radiation energy density is

$$\rho_{\text{R}} = \frac{\pi^2}{30} g_* T^4, \quad (30)$$

where g_* is the SM effective relativistic degrees of freedom.

Below we solve the set of Boltzmann equations by numerical methods. We assume that after reheating, all SM particles are in thermal equilibrium, while there are no N_i and ϕ particles because their interactions are too weak. Thus, the initial conditions can be set as $Y_\phi = Y_{N_1} = Y_{B-L} = 0$ at $x = 0.01$. Subsequently, ϕ particles are produced through interactions with SM Higgs bosons. For the interested parameter regions discussed below, they are nonrelativistic at relevant temperatures and hardly reach thermal equilibrium, so their energy density can be approximated by $\rho_\phi \simeq m_\phi n_\phi$.

Furthermore, $\langle \Gamma_i \rangle$ in the Boltzmann equations can be expressed as [83, 84]

$$\langle \Gamma_i \rangle = \frac{K_1(x)}{K_2(x)} \Gamma_i, \quad (31)$$

where $K_j(x)$ represents the the second kind modified Bessel function of order j . $\langle \sigma_{\phi\phi \rightarrow H\bar{H}} v \rangle$ can be calculated by [85, 86]

$$\langle \sigma_{\phi\phi \rightarrow H\bar{H}} v \rangle = \frac{T}{32\pi^4 (n_\phi^{\text{eq}})^2} \int_{4m_\phi^2}^{\infty} ds \sqrt{s} (s - 4m_\phi^2) \sigma_{\phi\phi \rightarrow H\bar{H}}(s) K_1\left(\frac{\sqrt{s}}{T}\right). \quad (32)$$

The washout effect in Eq. (28) is related to a factor of [84]

$$W_{\text{ID}}(x) = \frac{\langle \Gamma_{N_1} \rangle Y_{N_1}^{\text{eq}}}{2Hx Y_\ell^{\text{eq}}} = \frac{x K_1(x) \Gamma_N}{4H}. \quad (33)$$

When the ϕ decay processes are not effective, the energy density of nonrelativistic ϕ particles scale with the scale factor a as $\rho_\phi \propto a^{-3}$ because of the cosmic expansion. Compared with the radiation energy density $\rho_{\text{R}} \propto a^{-4}$, the dilution of ϕ particles are slower. Consequently, if the ϕ decay width is too small to deplete ϕ particles early enough, ρ_ϕ would soon dominate the universe, leading to an early matter-domination era that makes the evolution of the universe deviated from the standard Λ CDM model. This era ends after the ϕ decays become significant, i.e., $\langle \Gamma_\phi \rangle > H$, and additional entropy is injected by ϕ decays, heating up the plasma and increasing the photon number density n_γ . On the other hand, the generation of the lepton asymmetry arising from ϕ decays primarily depends on the ϕ number density rather than on the decay width Γ_ϕ . Consequently, the resulting $Y_{B-L} = n_{B-L}/n_\gamma$ decreases, leading to a reduction

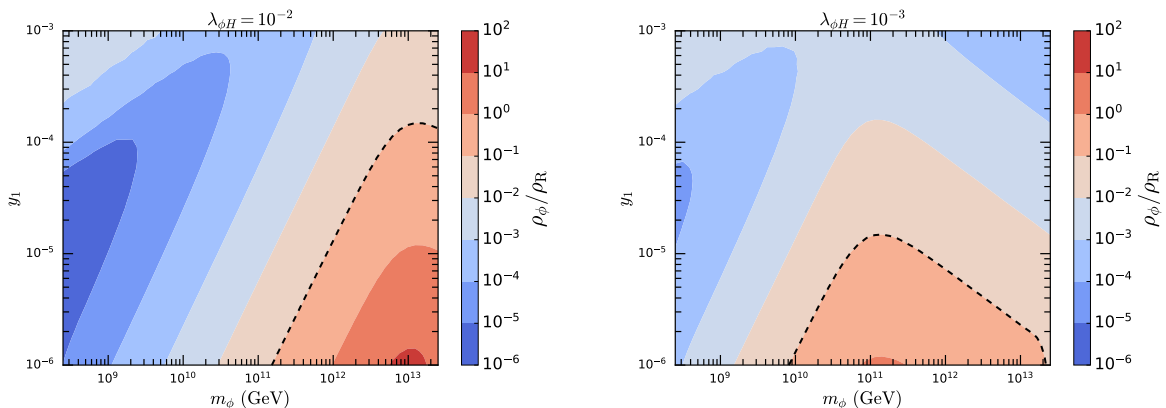


FIG. 3. Contours of ρ_ϕ/ρ_R when $\langle\Gamma_\phi\rangle = H$ for $\lambda_{\phi H} = 10^{-2}$ (left) and 10^{-3} (right). The other parameters are set to be $z = 0.2 + 0.2i$, $\kappa = 100\text{GeV}$, and $M_{N_1} = m_\phi/2.5$. The black dashed lines represent $\rho_\phi/\rho_R = 0.1$.

in the final baryon asymmetry η_B [87]. Such a dilution of the leptogenesis yield caused by entropy injection contradicts our goal of enhancing lepton asymmetry generation. Thus, we must prevent this situation by ensuring that the entropy injection from ϕ decays remains negligible. The ratio ρ_ϕ/ρ_R reaches the maximum roughly at the time with $\langle\Gamma_\phi\rangle = H$, after which it declines due to ϕ decays. Therefore, if we require $\rho_\phi/\rho_R < 0.1$ when $\langle\Gamma_\phi\rangle = H$, ϕ particles would never constitute a significant fraction of the total energy density of the universe, and the entropy injection into the plasma due to ϕ decays would be negligible.

In Fig. 3, we demonstrate the contours of ρ_ϕ/ρ_R when $\langle\Gamma_\phi\rangle = H$ in the m_ϕ - y_1 plane for $\lambda_{\phi H} = 10^{-2}$ and 10^{-3} , and the rest of parameters are fixed as $z = 0.2 + 0.2i$, $\kappa = 100\text{ GeV}$, and $M_{N_1} = m_\phi/2.5$. In the parameter regions with $\rho_\phi/\rho_R > 1$, there would be an early matter-domination era. For the $\lambda_{\phi H} = 10^{-2}$ case, this occurs at a region with $y_1 \lesssim 10^{-5}$ and $m_\phi \gtrsim 10^{12}\text{ GeV}$. For the $\lambda_{\phi H} = 10^{-3}$ case, the production rate of ϕ particles is lower, and ϕ particles can dominate the universe only in a small parameter region if $y_1 > 10^{-6}$. In the parameter regions with $\rho_\phi/\rho_R < 0.1$, the entropy injection from ϕ decays can be neglected, and this is the only situation we focus on in the following analysis.

We choose two benchmark points (BPs) for the model parameters, as outlined in the Table II. The Yukawa coupling matrix h_ν is determined by the Casas-Ibarra parametrization. We present the values of the h_ν elements, the CP asymmetry ε_1 , and the N_1 decay width Γ_{N_1} calculated for the two BPs in Table III. Compared to BP I with $z_i = 3$, BP II with $z_i = 0.3$ has a smaller CP asymmetry ε_1 and a much smaller Γ_{N_1} . Thus, the washout effect in BP II is expected to be much weaker than in BP I.

In order to evaluate the impact of the scalar ϕ , we separately demonstrate the evolution of number densities in the standard thermal leptogenesis without ϕ and that in the scalar-assisted leptogenesis. For the strong washout scheme BP I, Y_{N_1} , $|Y_{B-L}|$, and $(Y_{N_1} - Y_{N_1}^{\text{eq}})/Y_{N_1}^{\text{eq}}$ as functions of x in standard case are illustrated in left panel of Fig. 4, while Y_ϕ and Y_ϕ^{eq} are also plotted in the right panel of Fig. 4 for the scalar-assisted case.

TABLE II. Information for two BPs.

	M_{N_1} (GeV)	M_{N_2}	z_r	z_i	m_ϕ	y_1	κ (GeV)	$\lambda_{\phi H}$
BP I	10^{10}	$10M_{N_1}$	0.2	3	$2.5M_{N_1}$	3.22×10^{-5}	100	6.1×10^{-4}
BP II	5×10^9	$10M_{N_1}$	0.45	0.2	$2.5M_{N_1}$	3×10^{-5}	100	4.2×10^{-4}

TABLE III. Values of h_ν , ε_1 , and Γ_{N_1} for two BPs.

	h_ν	ε_1	Γ_{N_1} (GeV)
BP I	$\begin{pmatrix} 0.42 + 0.54i & -1.72 + 1.31i & 0.01 \\ 1.60 - 2.84i & 9.03 + 5.04i & 0 \\ -0.45 - 2.82i & 8.97 - 1.41i & 0 \end{pmatrix} \times 10^{-2}$	3.17×10^{-7}	7.67×10^5
BP II	$\begin{pmatrix} -0.01 + 0.40i & 0.54 - 1.75i & 0.05i \\ 0.37 + 1.60i & -1.07 + 5.26i & -0.02i \\ 0.44 + 0.18i & -0.17 + 6.39i & 0.03i \end{pmatrix} \times 10^{-3}$	2.03×10^{-7}	616.89

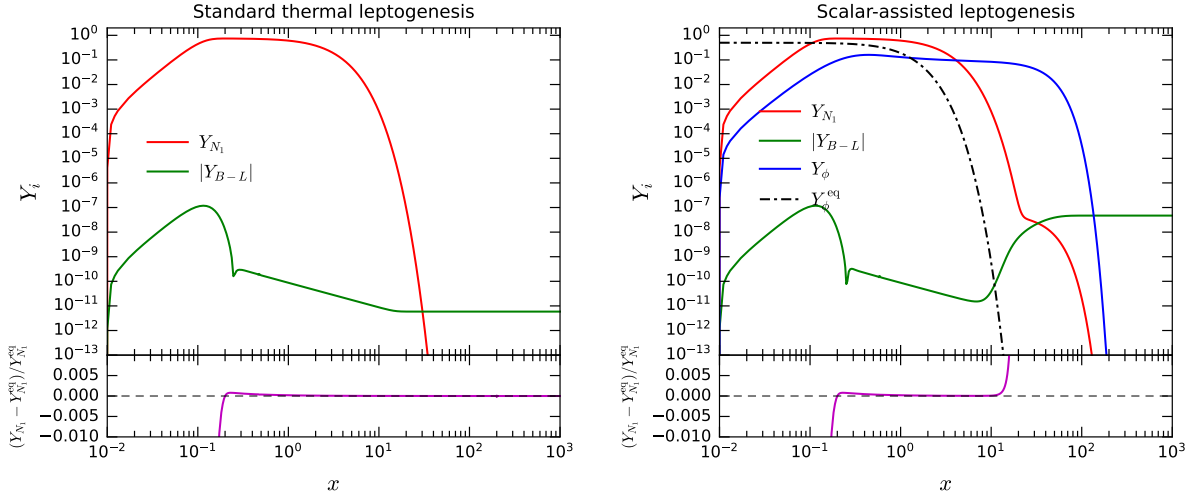


FIG. 4. Evolution of Y_{N_1} , Y_{B-L} , $(Y_{N_1} - Y_{N_1}^{\text{eq}})/Y_{N_1}^{\text{eq}}$, Y_ϕ , and Y_ϕ^{eq} as functions of $x = M_{N_1}/T$ in the standard (left) and scalar-assisted (right) leptogenesis for BP I, which is a strong washout scheme. The final baryon-to-photon ratios are $\eta_B = 7.36 \times 10^{-14}$ (left) and $\eta_B = 6.1 \times 10^{-10}$ (right).

In the standard case of BP I, although we have set a vanishing initial number density for N_1 , the N_1 particles are rapidly thermalized via interactions with the SM plasma, and Y_{N_1} quickly approaches the thermal value $Y_{N_1}^{\text{eq}}$. The CP -violating $N_1 \leftrightarrow \ell H/\bar{\ell} \bar{H}$ processes for nonzero $Y_{N_1} - Y_{N_1}^{\text{eq}}$ generate the lepton asymmetry, leading to the increase of $|Y_{B-L}|$ from $x = 0.01$. Then the washout processes begin to reduce the produced lepton asymmetry, resulting in the decrease of $|Y_{B-L}|$. There is a sharp change in the $|Y_{B-L}|$ curve at $x \sim 0.25$, and it corresponds to the sign flip of Y_{B-L} because the first negative $Y_{N_1} - Y_{N_1}^{\text{eq}}$ become positive after $x \sim 0.2$. For

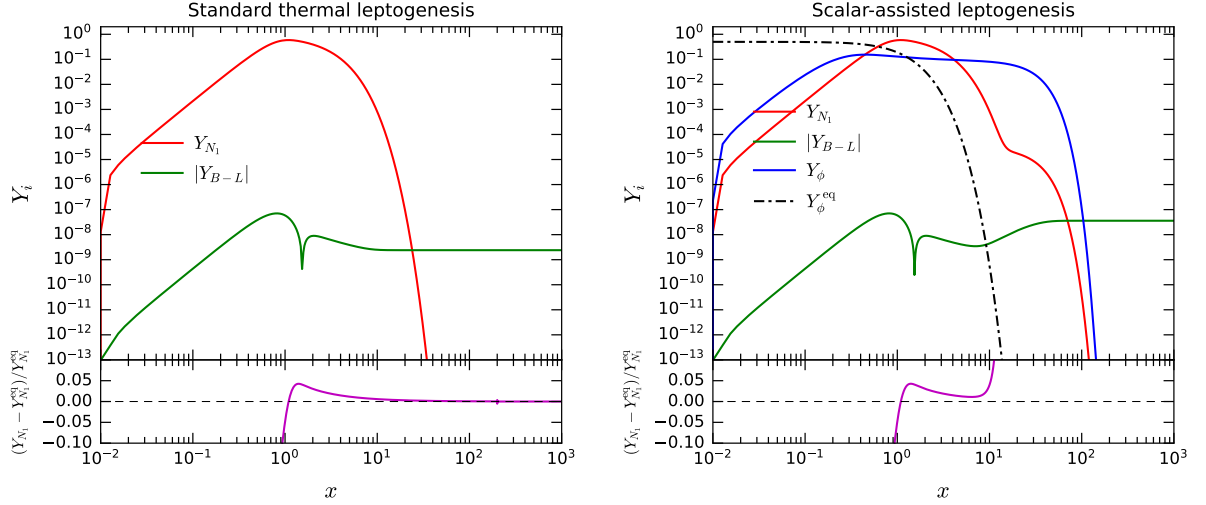


FIG. 5. Same as Fig. 4, but for BP II, which is a weak washout scheme. The final η_B are 3.12×10^{-11} (left) and 6.1×10^{-10} (right).

$x \gtrsim 0.25$, the net lepton numbers are regenerated under the competition between the generation and washout processes. The Y_{B-L} value tends to be steady for $x \gtrsim 20$, where both the generation and washout of the lepton symmetry are suppressed at such low temperatures. This leads to a final baryon-to-photon ratio of $\eta_B = 7.36 \times 10^{-14}$, which is too low to account for the observed value (1).

In the scalar-assisted case of BP I, the ϕ particles never reach thermal equilibrium. They are primarily produced at high temperatures through interactions with Higgs bosons, and finally dissipated by decay processes, among which the $\phi \rightarrow N_1 N_1$ decay leads to nonthermal production of N_1 particles. At low temperatures, such an extra source for the N_1 particles helps the generation of the lepton asymmetry. As demonstrated in the right panel of Fig. 4, $|Y_{B-L}|$ rises again at $x \sim 8$, and becomes constant for $x \gtrsim 60$, resulting in a final η_B of 6.1×10^{-10} to explain the observation.

Similarly, we present the results for the weak washout scheme BP II in Fig. 5. Compared with BP I, the small Γ_{N_1} in BP II slows down the thermalization of N_1 particles, and Y_{N_1} becomes close to $Y_{N_1}^{\text{eq}}$ at $x \sim 1$. A small Γ_{N_1} also implies a weak washout effect, and hence the decrease of $|Y_{B-L}|$ after $x \sim 2$ is quite slow. In the standard case, the final η_B is 3.12×10^{-11} , lower than the observed value by one order of magnitude. In the scalar-assisted case, $|Y_{B-L}|$ is lifted after $x \sim 10$, leading to a final η_B of 6.1×10^{-10} .

The discussions above show that the introduction of the scalar ϕ can effectively enhance the generation of the lepton asymmetry, especially in a strong washout scheme. Such an enhancement depends on the $\phi \rightarrow N_1 N_1$ decay width, which is proportional to the square of the Yukawa coupling y_1 . Meanwhile, the ϕ number density at the time of decay impacts on the outcome, and it means that the ϕ coupling to the Higgs field, $\lambda_{\phi H}$, also plays an important role. Below, we analyze the individual effects of y_1 and $\lambda_{\phi H}$ on the final baryon-to-photon ratio η_B .

In the left panel of Fig. 6, we show η_B as functions of y_1 for $z_1 = 0.1, 0.6$, and 1 with

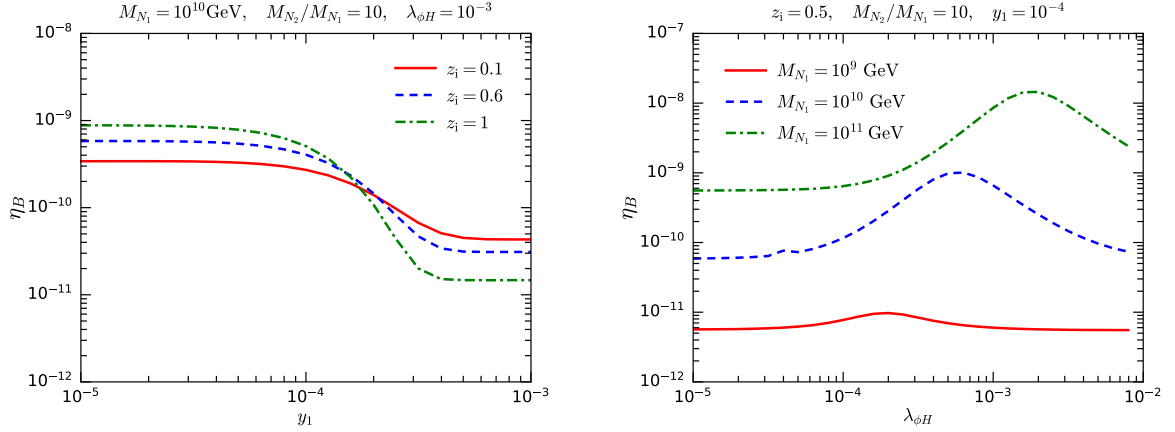


FIG. 6. The baryon-to-photon ratio η_B as functions of the Yukawa coupling y_1 for different values of z_i with $M_{N_1} = 10^{10}$ GeV and as functions of the quartic coupling $\lambda_{\phi H}$ for different values of M_{N_1} with $z_i = 0.5$ and $y_1 = 10^{-4}$ (right) in the scalar-assisted leptogenesis. The remaining parameters take the same values in BP II.

$M_{N_1} = 10^{10}$ GeV in the scalar-assisted leptogenesis. The values of the remaining parameters are the same as in BP II, including the mass relations $M_{N_2} = 10M_{N_1}$ and $m_\phi = 2.5M_{N_1}$. For a fixed z_i , it is observed that a smaller y_1 leads to a larger η_B , because ϕ particles with a longer lifetime would maintain a high number density for a longer time to produce more N_1 particles. For $y_1 \gtrsim 5 \times 10^{-4}$, the lifetime of the ϕ boson is too short to produce extra N_1 particles, and the resulting η_B are basically the same as in the standard leptogenesis. Note that a larger z_i means a larger washout effect, and the $z_i = 1$ case would lead to the lowest η_B among the three cases for $y_1 \gtrsim 5 \times 10^{-4}$. Nonetheless, for $y_1 \lesssim 2 \times 10^{-4}$, the ϕ decays could overcome the strong washout in the $z_i = 1$ case, making η_B comparable to or even larger than those in the other cases.

In the right panel of Fig. 6, we similarly demonstrate η_B as functions of $\lambda_{\phi H}$ for $M_{N_1} = 10^9$, 10^{10} , and 10^{11} GeV with $z_i = 0.1$, $y_1 = 10^{-4}$, and other parameters taking values in BP II. The choice of $y_1 = 10^{-4}$ ensures $\rho_\phi/\rho_R < 0.1$ when $\langle \Gamma_\phi \rangle = H$, maintaining the validity of our calculations. It clearly shows that $\lambda_{\phi H}$ also has a significant impact on the resulting lepton asymmetry, because the ϕ particles are produced through interactions with the SM Higgs bosons. If the $\phi\phi \rightarrow H\bar{H}$ cross section is too high, the number density of the remaining ϕ particles after $\phi\phi$ annihilation would be reduced. Conversely, if the cross section is too low, fewer ϕ particles will be generated at the beginning. Therefore, the strong enhancement of leptogenesis by the scalar decays appears at moderate values of $\lambda_{\phi H}$, such as $\lambda_{\phi H} \sim 2 \times 10^{-3}$ for $M_{N_1} = 10^{11}$ GeV and $\lambda_{\phi H} \sim 6 \times 10^{-4}$ for $M_{N_1} = 10^{10}$ GeV. Since we have fixed the relation $m_\phi = 2.5M_{N_1}$, for the case of $M_{N_1} = 10^9$ GeV, ϕ particles decay too early to make a notable contribution to η_B .

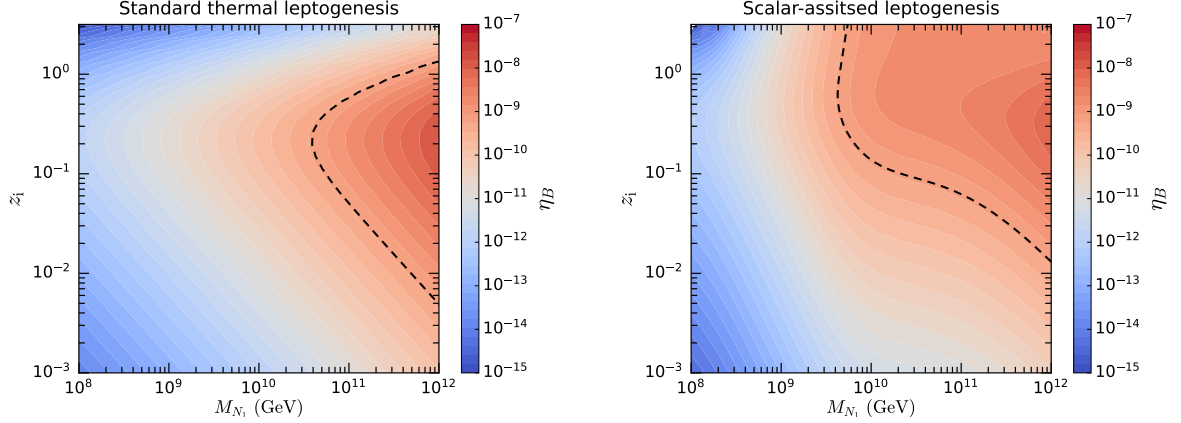


FIG. 7. η_B contours in the M_{N_1} - z_i plane for the standard (left) and scalar-assisted (right) leptogenesis with the remaining parameters taking the values in BP II. The dashed lines denote the observed value $\eta_B = 6.13 \times 10^{-10}$.

IV. PARAMETER SCANS

In order to understand the impact of the scalar ϕ , we perform some parameter scans in this section. Firstly, we conduct a scan in the M_{N_1} - z_i plane with $\lambda_{\phi H} = 10^{-4}$ and $y_1 = 10^{-4}$, while the rest of parameters take the values in BP II. Contours of η_B obtained in the standard and scalar-assisted leptogenesis are illustrated in the left and right panels of Fig. 7, respectively. Note that all the parameters points in Fig. 7 lead to $\rho_\phi/\rho_R < 0.1$ when $\langle \Gamma_\phi \rangle = H$.

In both cases, an increase in M_{N_1} implies an augmentation in the CP asymmetry ε_1 that essentially increases η_B . On the other hand, a larger z_i gives not only a larger ε_1 , but also a larger Γ_{N_1} , which would enhance the washout effect. Consequently, for a fixed M_{N_1} in the standard case, the resulting baryon-to-photon ratio increases as z_i increases from 10^{-3} , and reaches the maximum at $z_i \sim 0.2$, and then declines for larger z_i . In the scalar-assisted case, the nonthermal production of N_1 particles from ϕ decays can significantly increase the resulting η_B . In particular, it compensates the lepton asymmetry diminished by the strong washout for $z_i \gtrsim 0.2$. At $z_i \sim 1$, the value of M_{N_1} required for the correct η_B can be reduced by nearly two orders of magnitude, compared to the standard case.

Furthermore, we carry out a random scan within the following parameter ranges:

$$10^8 \text{ GeV} < M_{N_1} < 10^{10} \text{ GeV} \quad \text{with} \quad 10^{-5} < y_1 < 10^{-3}, \quad (34)$$

$$10^{10} \text{ GeV} < M_{N_1} < 10^{12} \text{ GeV} \quad \text{with} \quad 10^{-4} < y_1 < 10^{-3}, \quad (35)$$

$$10^{-3} < z_i < 3, \quad 0 < z_r < \pi/4, \quad 3 < M_{N_2}/M_{N_1} < 10^3, \quad (36)$$

$$10^{-3} \text{ GeV} < \kappa < 10^2 \text{ GeV}, \quad 10^{-5} < \lambda_{\phi H} < 10^{-2}. \quad (37)$$

Only the parameter points resulting in $\rho_\phi/\rho_R < 0.1$ when $\langle \Gamma_\phi \rangle = H$ are kept for the following analysis. In Fig. 8, we project the parameter points into the M_{N_1} - η_B plane with colors indicating the CP asymmetry ε_1 . It clearly shows that η_B is positively correlated to both M_{N_1} and ε_1 .

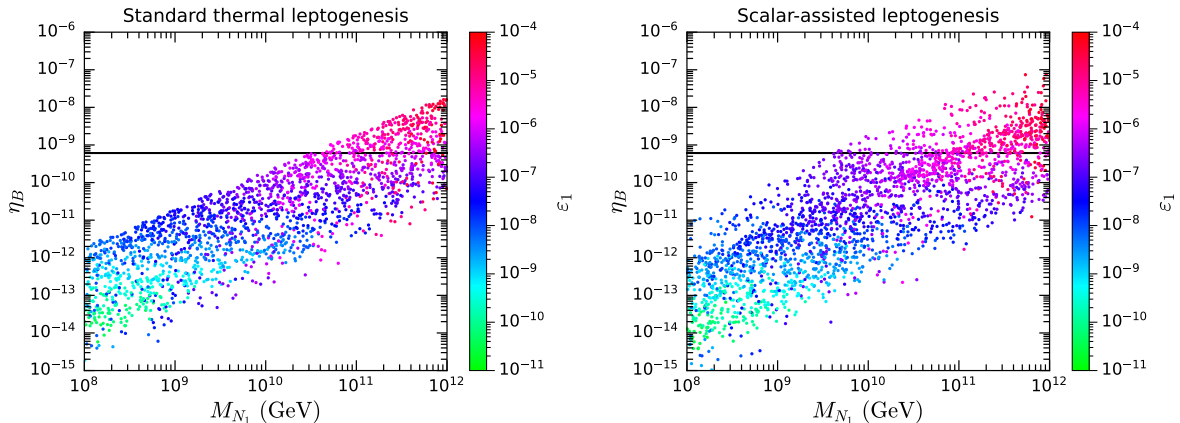


FIG. 8. Parameter points projected into the M_{N_1} - η_B plane for the standard (left) and scalar-assisted (right) leptogenesis. The color axes denote the CP asymmetry ϵ_1 , and the black horizontal lines indicate the observed value of the baryon-to-photon ratio.

In the standard leptogenesis, the observed baryon-to-photon ratio, which is denoted by the horizontal line, can be achieved for $M_{N_1} \gtrsim 3 \times 10^{10}$ GeV. On the other hand, as the scalar-assisted leptogenesis provides an extra nonthermal source for N_1 particles, the applicable value of M_{N_1} can be lowered down to $\sim 4 \times 10^9$ GeV for the correct η_B . Besides, the required values of ϵ_1 in the scalar-assisted case are smaller than the standard case.

In order to demonstrate the viable parameter ranges, we pick out the parameter points that lead to a baryon-to-photon ratio η_B within the 3σ range of the observational value (1). These parameter points are projected into the M_{N_1} - z_i and M_{N_1} - ϵ_1 planes, as illustrated in the left and right panels of Fig. 9, respectively. We find that the introduction of the scalar ϕ significantly enlarges the available parameter regions. Compared to the standard leptogenesis, the applicable M_{N_1} for the same z_i can be lowered down by one to three orders of magnitude. The lowest viable M_{N_1} is reduced from $\sim 3 \times 10^{10}$ GeV to $\sim 3 \times 10^9$ GeV, while the smallest viable ϵ_1 decreases from $\sim 6 \times 10^{-7}$ to $\sim 2 \times 10^{-7}$.

V. SUMMARY

In order to achieve the observed baryon asymmetry, the mass scale of RHNs in the standard leptogenesis should be rather high to provide a sufficient CP violation and to overcome the washout effect. In this work, we have proposed a particular scenario to lower down the RHN mass scale by introducing a scalar ϕ decaying into RHNs because of its Yukawa couplings. ϕ particles should have an adequate long lifetime so that their decays provide an additional nonthermal source for the RHNs after the washout effect is attenuated. Therefore, such a scalar-assisted leptogenesis can improve the generation of the lepton asymmetry, and the required RHN mass scale would be lower than the standard case.

To investigate the efficiency of our proposal, we have conducted a detailed analysis based on the one-flavor approximation, where only the $N_1 \leftrightarrow \ell H / \bar{\ell} \bar{H}$ processes are relevant to the

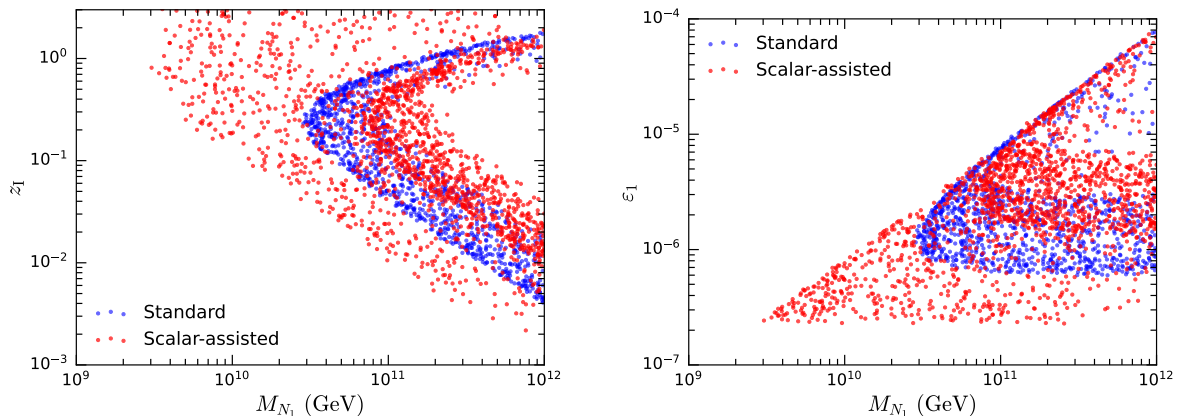


FIG. 9. Selected parameter points with the correct baryon-to-photon ratio projected into the M_{N_1} - z_i (left) and M_{N_1} - ε_1 (right) planes. The red and blue dots correspond to the standard and scalar-assisted leptogenesis, respectively.

generation of the lepton asymmetry. A set of Boltzmann equations describing the evolution of the related number densities are established and solved. The number densities as functions of $x = M_{N_1}/T$ are demonstrated for two BPs. For BP I with a strong washout effect, we have found that the inclusion of the scalar ϕ can lift up the final baryon-to-photon ratio η_B by four orders of magnitude, compared to the standard leptogenesis. For BP II with a weak washout effect, η_B can be increased by one order of magnitude in the scalar-assisted leptogenesis.

Furthermore, we have carried out parameter scans to explore the parameter space. A scan in the M_{N_1} - z_i plane with other parameters fixed shows that the resulting baryon asymmetry is widely increased in the scalar-assisted leptogenesis, especially in the parameter regions where the washout effect is strong. At $z_i \sim 1$, which leads to a very strong washout, the lightest RHN mass M_{N_1} required for the observed η_B can be lowered down by nearly two orders of magnitude. Based on a random scan in the parameter space, we have demonstrated the positive correlations of η_B to M_{N_1} and ε_1 , and that both the viable M_{N_1} and ε_1 in the scalar-assisted case are smaller than those in the standard case. Moreover, from the parameter points that are consistent with the observed baryon-to-photon ratio in the 3σ range, we have found that the scalar-assisted leptogenesis can effectively extend the available parameter ranges, lowering down the viable M_{N_1} by one to three orders of magnitude for the same z_i .

These results clearly show that the scalar-assisted leptogenesis is a feasible avenue to lower down the RHN mass scale, particularly when the washout effect is strong. A lower mass scale may more easily be related to rich phenomena that can be tested in experiments. Potential implications of our work may extend beyond the specific model investigated here, offering valuable insights into the leptogenesis mechanism in diverse theoretical frameworks. Since there are a lot of extra scalar fields in new physics beyond the SM, the origin of the scalar ϕ could be linked to other interesting topics, such as the origin of dark matter, grand unification, supersymmetry, and so on.

ACKNOWLEDGMENTS

This work is supported by the National Natural Science Foundation of China (NSFC) under Grants No. 12275367 and No. 11875327, the Fundamental Research Funds for the Central Universities, the Guangzhou Science and Technology Planning Project under Grants No. 2024A04J4026, and the Sun Yat-Sen University Science Foundation.

-
- [1] A. G. Cohen, A. De Rujula, and S. L. Glashow, “A Matter - antimatter universe?,” *Astrophys. J.* **495** (1998) 539–549, [arXiv:astro-ph/9707087](#).
 - [2] **Planck** Collaboration, N. Aghanim *et al.*, “Planck 2018 results. I. Overview and the cosmological legacy of Planck,” *Astron. Astrophys.* **641** (2020) A1, [arXiv:1807.06205 \[astro-ph.CO\]](#).
 - [3] B. D. Fields, K. A. Olive, T.-H. Yeh, and C. Young, “Big-Bang Nucleosynthesis after Planck,” *JCAP* **03** (2020) 010, [arXiv:1912.01132 \[astro-ph.CO\]](#). [Erratum: JCAP 11, E02 (2020)].
 - [4] A. D. Sakharov, “Violation of CP Invariance, C asymmetry, and baryon asymmetry of the universe,” *Pisma Zh. Eksp. Teor. Fiz.* **5** (1967) 32–35.
 - [5] G. ’t Hooft, “Symmetry Breaking Through Bell-Jackiw Anomalies,” *Phys. Rev. Lett.* **37** (1976) 8–11.
 - [6] V. A. Rubakov and M. E. Shaposhnikov, “Electroweak baryon number nonconservation in the early universe and in high-energy collisions,” *Usp. Fiz. Nauk* **166** (1996) 493–537, [arXiv:hep-ph/9603208](#).
 - [7] V. A. Kuzmin, V. A. Rubakov, and M. E. Shaposhnikov, “On the Anomalous Electroweak Baryon Number Nonconservation in the Early Universe,” *Phys. Lett. B* **155** (1985) 36.
 - [8] W. Buchmuller and O. Philipsen, “Phase structure and phase transition of the SU(2) Higgs model in three-dimensions,” *Nucl. Phys. B* **443** (1995) 47–69, [arXiv:hep-ph/9411334](#).
 - [9] K. Kajantie, M. Laine, K. Rummukainen, and M. E. Shaposhnikov, “Is there a hot electroweak phase transition at $m_H \gtrsim m_W$?,” *Phys. Rev. Lett.* **77** (1996) 2887–2890, [arXiv:hep-ph/9605288](#).
 - [10] F. Csikor, Z. Fodor, and J. Heitger, “Endpoint of the hot electroweak phase transition,” *Phys. Rev. Lett.* **82** (1999) 21–24, [arXiv:hep-ph/9809291](#).
 - [11] M. Dine and A. Kusenko, “The Origin of the matter - antimatter asymmetry,” *Rev. Mod. Phys.* **76** (2003) 1, [arXiv:hep-ph/0303065](#).
 - [12] D. Bodeker and W. Buchmuller, “Baryogenesis from the weak scale to the grand unification scale,” *Rev. Mod. Phys.* **93** (2021) 035004, [arXiv:2009.07294 \[hep-ph\]](#).
 - [13] D. S. Pereira, J. a. Ferraz, F. S. N. Lobo, and J. P. Mimoso, “Baryogenesis: A Symmetry Breaking in the Primordial Universe Revisited,” *Symmetry* **16** (2024) 13, [arXiv:2312.14080 \[gr-qc\]](#).
 - [14] M. Fukugita and T. Yanagida, “Baryogenesis Without Grand Unification,” *Phys. Lett. B* **174** (1986) 45–47.
 - [15] M. A. Luty, “Baryogenesis via leptogenesis,” *Phys. Rev. D* **45** (1992) 455–465.
 - [16] P. Minkowski, “ $\mu \rightarrow e\gamma$ at a Rate of One Out of 10^9 Muon Decays?,” *Phys. Lett. B* **67** (1977) 421–428.
 - [17] M. Gell-Mann, P. Ramond, and R. Slansky, “Complex Spinors and Unified Theories,” *Conf. Proc. C* **790927** (1979) 315–321, [arXiv:1306.4669 \[hep-th\]](#).
 - [18] T. Yanagida, “Horizontal gauge symmetry and masses of neutrinos,” *Conf. Proc. C* **7902131** (1979) 95–99.

- [19] A. Kusenko, K. Schmitz, and T. T. Yanagida, “Leptogenesis via Axion Oscillations after Inflation,” *Phys. Rev. Lett.* **115** (2015) 011302, [arXiv:1412.2043 \[hep-ph\]](#).
- [20] L. Pearce, L. Yang, A. Kusenko, and M. Peloso, “Leptogenesis via neutrino production during Higgs condensate relaxation,” *Phys. Rev. D* **92** (2015) 023509, [arXiv:1505.02461 \[hep-ph\]](#).
- [21] S. Pascoli, J. Turner, and Y.-L. Zhou, “Baryogenesis via leptonic CP-violating phase transition,” *Phys. Lett. B* **780** (2018) 313–318, [arXiv:1609.07969 \[hep-ph\]](#).
- [22] K. Agashe, P. Du, M. Ekhterachian, C. S. Fong, S. Hong, and L. Vecchi, “Hybrid seesaw leptogenesis and TeV singlets,” *Phys. Lett. B* **785** (2018) 489–497, [arXiv:1804.06847 \[hep-ph\]](#).
- [23] N. D. Barrie, C. Han, and H. Murayama, “Affleck-Dine Leptogenesis from Higgs Inflation,” *Phys. Rev. Lett.* **128** (2022) 141801, [arXiv:2106.03381 \[hep-ph\]](#).
- [24] J. Berman, B. Shuve, and D. Tucker-Smith, “Freeze-in leptogenesis via dark-matter oscillations,” *Phys. Rev. D* **105** (2022) 095027, [arXiv:2201.11502 \[hep-ph\]](#).
- [25] S. Bhattacharya, R. Roshan, A. Sil, and D. Vatsyayan, “Symmetry origin of baryon asymmetry, dark matter, and neutrino mass,” *Phys. Rev. D* **106** (2022) 075005, [arXiv:2105.06189 \[hep-ph\]](#).
- [26] E. Fernández-Martínez, X. Marcano, and D. Naredo-Tuero, “HNL mass degeneracy: implications for low-scale seesaws, LNV at colliders and leptogenesis,” *JHEP* **03** (2023) 057, [arXiv:2209.04461 \[hep-ph\]](#).
- [27] J. Carrasco-Martínez, D. I. Dunsky, L. J. Hall, and K. Harigaya, “Leptogenesis in Parity Solutions to the Strong CP Problem and Standard Model Parameters,” [arXiv:2307.15731 \[hep-ph\]](#).
- [28] A. Datta, R. Roshan, and A. Sil, “Scalar triplet flavor leptogenesis with dark matter,” *Phys. Rev. D* **105** (2022) 095032, [arXiv:2110.03914 \[hep-ph\]](#).
- [29] R. T. Co and K. Harigaya, “Axiogenesis,” *Phys. Rev. Lett.* **124** (2020) 111602, [arXiv:1910.02080 \[hep-ph\]](#).
- [30] Z.-h. Zhao, “Renormalization group evolution induced leptogenesis in the minimal seesaw model with the trimaximal mixing and mu-tau reflection symmetry,” *JHEP* **11** (2021) 170, [arXiv:2003.00654 \[hep-ph\]](#).
- [31] S. Enomoto, C. Cai, Z.-H. Yu, and H.-H. Zhang, “Leptogenesis due to oscillating Higgs field,” *Eur. Phys. J. C* **80** (2020) 1098, [arXiv:2005.08037 \[hep-ph\]](#).
- [32] X.-M. Jiang, Y.-L. Tang, Z.-H. Yu, and H.-H. Zhang, “ $1 \leftrightarrow 2$ processes of a sterile neutrino around the electroweak scale in a thermal plasma,” *Phys. Rev. D* **103** (2021) 095003, [arXiv:2008.00642 \[hep-ph\]](#).
- [33] A. Dutta Banik, R. Roshan, and A. Sil, “Neutrino mass and asymmetric dark matter: study with inert Higgs doublet and high scale validity,” *JCAP* **03** (2021) 037, [arXiv:2011.04371 \[hep-ph\]](#).
- [34] A. Granelli, K. Hamaguchi, N. Nagata, M. E. Ramirez-Quezada, and J. Wada, “Thermal leptogenesis in the minimal gauged $U(1)_{L_\mu-L_\tau}$ model,” *JHEP* **09** (2023) 079, [arXiv:2305.18100 \[hep-ph\]](#).
- [35] S.-L. Chen, Z. Kang, Z.-K. Liu, and P. Zhang, “Matter Asymmetries in the Z_N Dark matter-companion Models,” [arXiv:2405.05694 \[hep-ph\]](#).
- [36] S. Davidson and A. Ibarra, “A Lower bound on the right-handed neutrino mass from leptogenesis,” *Phys. Lett. B* **535** (2002) 25–32, [arXiv:hep-ph/0202239](#).
- [37] W. Buchmuller, P. Di Bari, and M. Plumacher, “Cosmic microwave background, matter - antimatter asymmetry and neutrino masses,” *Nucl. Phys. B* **643** (2002) 367–390, [arXiv:hep-ph/0205349](#). [Erratum: Nucl.Phys.B 793, 362 (2008)].
- [38] W. Buchmuller, P. Di Bari, and M. Plumacher, “A Bound on neutrino masses from baryogenesis,” *Phys. Lett. B* **547** (2002) 128–132, [arXiv:hep-ph/0209301](#).
- [39] W. Buchmuller, P. Di Bari, and M. Plumacher, “The Neutrino mass window for baryogenesis,”

- Nucl. Phys. B* **665** (2003) 445–468, [arXiv:hep-ph/0302092](#).
- [40] T. Asaka, K. Hamaguchi, M. Kawasaki, and T. Yanagida, “Leptogenesis in inflaton decay,” *Phys. Lett. B* **464** (1999) 12–18, [arXiv:hep-ph/9906366](#).
 - [41] F. Hahn-Woernle and M. Plumacher, “Effects of reheating on leptogenesis,” *Nucl. Phys. B* **806** (2009) 68–83, [arXiv:0801.3972 \[hep-ph\]](#).
 - [42] B. Barman, D. Borah, and R. Roshan, “Nonthermal leptogenesis and UV freeze-in of dark matter: Impact of inflationary reheating,” *Phys. Rev. D* **104** (2021) 035022, [arXiv:2103.01675 \[hep-ph\]](#).
 - [43] V. Domcke, K. Kamada, K. Mukaida, K. Schmitz, and M. Yamada, “Wash-In Leptogenesis,” *Phys. Rev. Lett.* **126** (2021) 201802, [arXiv:2011.09347 \[hep-ph\]](#).
 - [44] V. Domcke, K. Kamada, K. Mukaida, K. Schmitz, and M. Yamada, “Wash-in leptogenesis after axion inflation,” *JHEP* **01** (2023) 053, [arXiv:2210.06412 \[hep-ph\]](#).
 - [45] S. Datta, A. Ghosal, and R. Samanta, “Baryogenesis from ultralight primordial black holes and strong gravitational waves from cosmic strings,” *JCAP* **08** (2021) 021, [arXiv:2012.14981 \[hep-ph\]](#).
 - [46] B. Barman, D. Borah, S. J. Das, and R. Roshan, “Non-thermal origin of asymmetric dark matter from inflaton and primordial black holes,” *JCAP* **03** (2022) 031, [arXiv:2111.08034 \[hep-ph\]](#).
 - [47] R. Calabrese, M. Chianese, J. Gunn, G. Miele, S. Morisi, and N. Saviano, “Limits on light primordial black holes from high-scale leptogenesis,” *Phys. Rev. D* **107** (2023) 123537, [arXiv:2305.13369 \[hep-ph\]](#).
 - [48] K. Schmitz and X.-J. Xu, “Wash-in leptogenesis after the evaporation of primordial black holes,” [arXiv:2311.01089 \[hep-ph\]](#).
 - [49] A. Ghoshal, Y. F. Perez-Gonzalez, and J. Turner, “Superradiant Leptogenesis,” [arXiv:2312.06768 \[hep-ph\]](#).
 - [50] D. Suematsu, “Low scale leptogenesis in a hybrid model of the scotogenic type I and III seesaw models,” *Phys. Rev. D* **100** (2019) 055008, [arXiv:1906.12008 \[hep-ph\]](#).
 - [51] P. Huang and T. Xu, “Leptogenesis with a Coupling Knob,” [arXiv:2312.06380 \[hep-ph\]](#).
 - [52] E. J. Chun, T. P. Dutka, T. H. Jung, X. Nagels, and M. Vanvlasselaer, “Bubble-assisted leptogenesis,” *JHEP* **09** (2023) 164, [arXiv:2305.10759 \[hep-ph\]](#).
 - [53] M. Dehpour, “Thermal leptogenesis in nonextensive cosmology,” *Eur. Phys. J. C* **84** (2024) 340, [arXiv:2401.00229 \[hep-ph\]](#).
 - [54] M. Dehpour, “Thermal leptogenesis in anisotropic cosmology,” *Int. J. Mod. Phys. A* **38** (2023) 2350181, [arXiv:2312.10677 \[hep-ph\]](#).
 - [55] A. Pilaftsis and T. E. J. Underwood, “Resonant leptogenesis,” *Nucl. Phys. B* **692** (2004) 303–345, [arXiv:hep-ph/0309342](#).
 - [56] A. Pilaftsis, “Resonant tau-leptogenesis with observable lepton number violation,” *Phys. Rev. Lett.* **95** (2005) 081602, [arXiv:hep-ph/0408103](#).
 - [57] B. Dev, M. Garny, J. Klaric, P. Millington, and D. Teresi, “Resonant enhancement in leptogenesis,” *Int. J. Mod. Phys. A* **33** (2018) 1842003, [arXiv:1711.02863 \[hep-ph\]](#).
 - [58] P. C. da Silva, D. Karamitros, T. McKelvey, and A. Pilaftsis, “Tri-resonant leptogenesis in a seesaw extension of the Standard Model,” *JHEP* **11** (2022) 065, [arXiv:2206.08352 \[hep-ph\]](#).
 - [59] D. Karamitros, T. McKelvey, and A. Pilaftsis, “Varying entropy degrees of freedom effects in low-scale leptogenesis,” *Phys. Rev. D* **109** (2024) 055007, [arXiv:2310.03703 \[hep-ph\]](#).
 - [60] Z.-h. Zhao, J. Zhang, and X.-Y. Wu, “Flavored leptogenesis from a sudden mass gain of right-handed neutrinos,” [arXiv:2403.18630 \[hep-ph\]](#).
 - [61] R. Barbieri, P. Creminelli, A. Strumia, and N. Tetradis, “Baryogenesis through leptogenesis,” *Nucl. Phys. B* **575** (2000) 61–77, [arXiv:hep-ph/9911315](#).

- [62] A. Abada, S. Davidson, A. Ibarra, F. X. Josse-Michaux, M. Losada, and A. Riotto, “Flavour Matters in Leptogenesis,” *JHEP* **09** (2006) 010, [arXiv:hep-ph/0605281](#).
- [63] K. Moffat, S. Pascoli, S. T. Petcov, H. Schulz, and J. Turner, “Three-flavored nonresonant leptogenesis at intermediate scales,” *Phys. Rev. D* **98** (2018) 015036, [arXiv:1804.05066 \[hep-ph\]](#).
- [64] T. Alanne, T. Hugle, M. Platscher, and K. Schmitz, “Low-scale leptogenesis assisted by a real scalar singlet,” *JCAP* **03** (2019) 037, [arXiv:1812.04421 \[hep-ph\]](#).
- [65] P. S. B. Dev, R. N. Mohapatra, and Y. Zhang, “Leptogenesis constraints on $B - L$ breaking Higgs boson in TeV scale seesaw models,” *JHEP* **03** (2018) 122, [arXiv:1711.07634 \[hep-ph\]](#).
- [66] D. M. Barreiros, H. B. Câmara, R. G. Felipe, and F. R. Joaquim, “Scalar-singlet assisted leptogenesis with CP violation from the vacuum,” *JHEP* **01** (2023) 010, [arXiv:2211.00042 \[hep-ph\]](#).
- [67] J. A. Casas and A. Ibarra, “Oscillating neutrinos and $\mu \rightarrow e, \gamma$,” *Nucl. Phys. B* **618** (2001) 171–204, [arXiv:hep-ph/0103065](#).
- [68] B. Pontecorvo, “Inverse beta processes and nonconservation of lepton charge,” *Zh. Eksp. Teor. Fiz.* **34** (1957) 247.
- [69] Z. Maki, M. Nakagawa, and S. Sakata, “Remarks on the unified model of elementary particles,” *Prog. Theor. Phys.* **28** (1962) 870–880.
- [70] **Particle Data Group** Collaboration, R. L. Workman and Others, “Review of Particle Physics,” *PTEP* **2022** (2022) 083C01.
- [71] M. C. Gonzalez-Garcia, M. Maltoni, and T. Schwetz, “NuFIT: Three-Flavour Global Analyses of Neutrino Oscillation Experiments,” *Universe* **7** (2021) 459, [arXiv:2111.03086 \[hep-ph\]](#).
- [72] S. Antusch, P. Di Bari, D. A. Jones, and S. F. King, “Leptogenesis in the Two Right-Handed Neutrino Model Revisited,” *Phys. Rev. D* **86** (2012) 023516, [arXiv:1107.6002 \[hep-ph\]](#).
- [73] L. Covi, E. Roulet, and F. Vissani, “CP violating decays in leptogenesis scenarios,” *Phys. Lett. B* **384** (1996) 169–174, [arXiv:hep-ph/9605319](#).
- [74] S. Y. Khlebnikov and M. E. Shaposhnikov, “The Statistical Theory of Anomalous Fermion Number Nonconservation,” *Nucl. Phys. B* **308** (1988) 885–912.
- [75] E. W. Kolb and M. S. Turner, *The Early Universe*, vol. 69. 1990.
- [76] Z.-Z. Xing and S. Zhou, *Neutrinos in particle physics, astronomy and cosmology*. Springer, 2011.
- [77] A. Basboll and S. Hannestad, “Decay of heavy Majorana neutrinos using the full Boltzmann equation including its implications for leptogenesis,” *JCAP* **01** (2007) 003, [arXiv:hep-ph/0609025](#).
- [78] J. Garayoa, S. Pastor, T. Pinto, N. Rius, and O. Vives, “On the full Boltzmann equations for Leptogenesis,” *JCAP* **09** (2009) 035, [arXiv:0905.4834 \[hep-ph\]](#).
- [79] F. Hahn-Woernle, M. Plumacher, and Y. Y. Y. Wong, “Full Boltzmann equations for leptogenesis including scattering,” *JCAP* **08** (2009) 028, [arXiv:0907.0205 \[hep-ph\]](#).
- [80] S. Hofmann, D. J. Schwarz, and H. Stoecker, “Damping scales of neutralino cold dark matter,” *Phys. Rev. D* **64** (2001) 083507, [arXiv:astro-ph/0104173](#).
- [81] L. Visinelli and P. Gondolo, “Kinetic decoupling of WIMPs: analytic expressions,” *Phys. Rev. D* **91** (2015) 083526, [arXiv:1501.02233 \[astro-ph.CO\]](#).
- [82] C. Cai and H.-H. Zhang, “Vector dark matter production from catalyzed annihilation,” *JHEP* **01** (2022) 099, [arXiv:2107.13475 \[hep-ph\]](#).
- [83] E. W. Kolb and S. Wolfram, “Baryon Number Generation in the Early Universe,” *Nucl. Phys. B* **172** (1980) 224. [Erratum: *Nucl.Phys.B* 195, 542 (1982)].
- [84] W. Buchmuller, P. Di Bari, and M. Plumacher, “Leptogenesis for pedestrians,” *Annals Phys.* **315** (2005) 305–351, [arXiv:hep-ph/0401240](#).

- [85] P. Gondolo and G. Gelmini, “Cosmic abundances of stable particles: Improved analysis,” *Nucl. Phys. B* **360** (1991) 145–179.
- [86] M. Plumacher, “Baryon asymmetry, neutrino mixing and supersymmetric SO(10) unification,” *Nucl. Phys. B* **530** (1998) 207–246, [arXiv:hep-ph/9704231](#).
- [87] M. Cataldi, A. Mariotti, F. Sala, and M. Vanvlasselaer, “ALP leptogenesis: non-thermal right-handed neutrinos from axions,” *JHEP* **12** (2024) 125, [arXiv:2407.01667 \[hep-ph\]](#).